Available online at www.sciencedirect.com
ScienceDirect
Tectonophysics 423 (2006) 3–16
TECTONOPHYSICS
www.elsevier.com/locate/tecto

Spatio-temporal microseismicity clustering in the Cretan region

Dirk Becker [a,*], Thomas Meier [a], Martina Rische [a], Marco Bohnhoff [b], Hans-Peter Harjes [a]

[a] *Department of Geosciences, Ruhr-University Bochum, Germany*
[b] *GeoForschungsZentrum Potsdam, Germany*

Received 30 March 2005; received in revised form 14 September 2005; accepted 25 March 2006
Available online 6 June 2006

Abstract

Spatio-temporal clustering of microseismicity in the central forearc of the Hellenic Subduction Zone in the area of Crete is investigated. Data for this study were gathered by temporary short period networks which were installed on the islands of Crete and Gavdos between 1996 and 2004. The similarity of waveforms is quantified systematically to identify clusters of microseismicity. Waveform similarities are calculated using an adaptive time window containing both the P- and S-wave onsets. The cluster detection is performed by applying a single linkage approach. Clusters are found in the interplate seismicity as well as in the intraplate seismicity of the continental crust in the region of the transtensional Ptolemy structure. The majority of the clusters are off the southern coast of Crete, in a region of elevated intraplate microseismic activity within the Aegean plate. Clusters in the Gavdos region are located at depths compatible with the plate interface while cluster activity in the region of the Ptolemy trench is distributed along a nearly vertical structure throughout the crust extending down to the plate interface. Most clusters show swarm-like behaviour with seismic activity confined to only a few hours or days, without a dominant earthquake and with a power law distribution of the interevent times.

For the largest cluster, precise relocations of the events using travel time differences of P- and S-waves derived from waveform cross correlations reveal migration of the hypocenters. This cluster is located in the region of the Ptolemy trench and migration occurs along the strike of the trench at ~500 m/day.

Relocated hypocenters as well as subtle differences in the waveforms suggest an offset between the hypocenters and thus the activation of distinct patches on the rupture surface. The observed microseismicity patterns may be related to fluids being transported along the plate interface and escaping towards the surface in zones of crustal weakness (Ptolemy structure), triggering swarm-like cluster activity along its way.

Keywords: Hellenic Subduction Zone; Microseismicity; Earthquake swarms; Fluid migration

1. Introduction

1.1. Region

The Hellenic Subduction Zone is the most seismically active region in Europe. It currently shows a high level of intermediate magnitude activity but it has also generated events with magnitudes up to 8.3 in historic times

* Corresponding author. Ruhr University Bochum, Institute of Geology, Mineralogy and Geophysics, NA 3/172, Universitaetsstr, 150, 44780 Bochum, Germany. Tel.: +49 234 3223275; fax: +49 234 3214181.
E-mail address: becker@geophysik.ruhr-uni-bochum.de (D. Becker).

0040-1951/$ - see front matter © 2006 Elsevier B.V. All rights reserved.
doi:10.1016/j.tecto.2006.03.022

(Papazachos et al., 2000; Stiros, 2001) (Fig. 1). The coupling of the subduction interface seems to be weak however with a large amount of slip being accommodated aseismically (e.g. North, 1974; Papadopoulos, 1989; Jenny et al., 2004; Becker et al., 2004). The general tectonic regime (McKenzie, 1970; LePichon et al., 1995) in the region is influenced by the extrusion and counterclockwise rotation of the Anatolian–Aegean region, the slow northward movement of Africa with respect to Eurasia (McClusky et al., 2000) and slab rollback caused by slab pull of the downgoing African slab. However, the thinned continental crust which constitutes the Southern Aegean north of Crete shows little internal deformation (McClusky et al., 2000; Kreemer and Chamot-Rooke, 2004). The relative movement between the southern Aegean and Eurasia is concentrated in the Northern Aegean Sea and along the Gulf of Corinth (McClusky et al., 2000). In the forearc, the Hellenic trench system consisting of the Ionian trench in the west and the Ptolemy, Pliny and Strabo trenches in the east, represent structures in the overriding Aegean lithosphere (Fig. 1). These transtensional features may be caused by sinistral movements of forearc slivers relative to the Aegean region due to increasingly oblique subduction towards the eastern forearc (ten Veen and Kleinspehn, 2003; Meier et al., 2004). Seismic refraction profiles (Bohnhoff et al., 2001) show a 4 km deep, wedge-shaped sedimentary structure in the Ptolemy trench supporting this interpretation.

Benioff zone seismicity in the east can be traced down to depths of about 160 km beneath Kos while seismicity in the shallower dipping western segment terminates at approximately 100 km below Milos. Large historic earthquakes are reported for the Cretan Sea north of Crete as well as for the plate interface south of the island (Fig. 1). Recent tectonic uplift of Crete with especially high rates in the western part of the island (Meulenkamp et al., 1994; Lambeck, 1995) is a further noteworthy point. Several studies have dealt with the microseismic activity in the Cretan region based on the evaluation of data from temporary dense seismic networks (e.g. de Chabalier et al., 1992; Hatzfeld et al., 1993; Delibasis et al., 1999; Becker, 2000; Meier et al., 2004). These studies identified and mapped the plate contact between the African and Aegean plates as well as the currently active structures

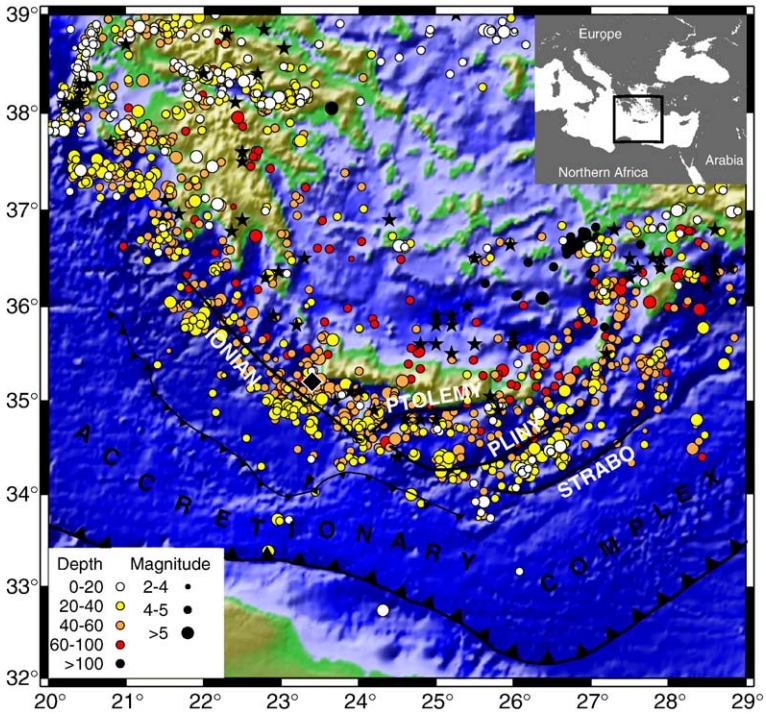

Fig. 1. General tectonic setting of the research area. Solid black lines indicate the transtensional structures south-east of Crete (Ptolemy, Pliny, Strabo) and the western deep-sea trench (Ionian), respectively. Thick line with triangles indicates the southern border of the accretionary complex while the thin line with triangles indicates the border between the outer and inner units of the accretionary complex which coincides with the presumed location of the crustal ocean–continent transition. Filled circles indicate relocated ISC seismicity from 1964 to 1998 (Engdahl et al., 1998) while black stars indicate historic seismicity with M_w=7.0 or greater for the time period from 550 BC to 1999 AD (Papazachos et al., 2000). Diamond indicates location of M_w=8.3 event in 365 AD.

within the continental crust. They found abundant microseismic activity in the southern offshore region, especially in the Ptolemy structure, as well as at the plate contact and within the top 20 km of the continental crust below Crete, while the microseismic activity in the depth range between 20 and 40 km below Crete and the Cretan Sea north of Crete is comparatively low (Meier et al., 2004).

In this paper we examine whether the microseismicity in the forearc of the central Hellenic Subduction Zone occurs in clusters. The aim is to detect and interpret zones of cluster activity within seismogenic structures of the forearc region.

1.2. Cluster

The occurrence of events with highly similar waveforms is well documented for regions with strike-slip regimes (e.g. Nadeau et al., 1995) and volcanic regions (e.g. Got et al., 1994). For the northeastern Japan subduction zone Igarashi et al. (2003) used similar events with magnitudes larger than 3 to investigate the distribution of slip on the subducting surface.

Repeating events with nearly constant interevent time and an almost identical magnitude (Nadeau et al., 1995; Nadeau and Johnson, 1998; Igarashi et al., 2003) can be distinguished from a sequence of similar events occurring during swarm-like activity lasting hours or days. This swarm-like activity can either occur within the aftershock sequence of a larger event following the Omori law for aftershocks (Schaff and Beroza, 2004) or during the microseismic activity of an earthquake swarm without a major shock. Such swarm-like activity is generally linked to the presence of fluids (e.g. Yamashita, 1999; Parotidis et al., 2003; Kurz et al., 2004) while repeating events are usually attributed to the effect of tectonic loading (Nadeau and McEvilly, 1997).

The high waveform similarity of such events suggests a close spatial proximity of the seismic activity and makes them candidates for precise relative relocation techniques in order to delineate the structures activated. Shearer (2002) and Rubin et al. (1999) used this approach to locate streaks of similar events in California, while Got et al. (1994) inferred a dipping fault-plane below Kilauea volcano and Gillard et al. (1996) found narrow bands of seismicity below Kilauea volcano. In volcanic and hydrothermal regions the relocation technique has also been applied to image magma movement (Hayashi and Morita, 2003) and fluid migration (Spicak and Horalek, 2001) related to swarm activity.

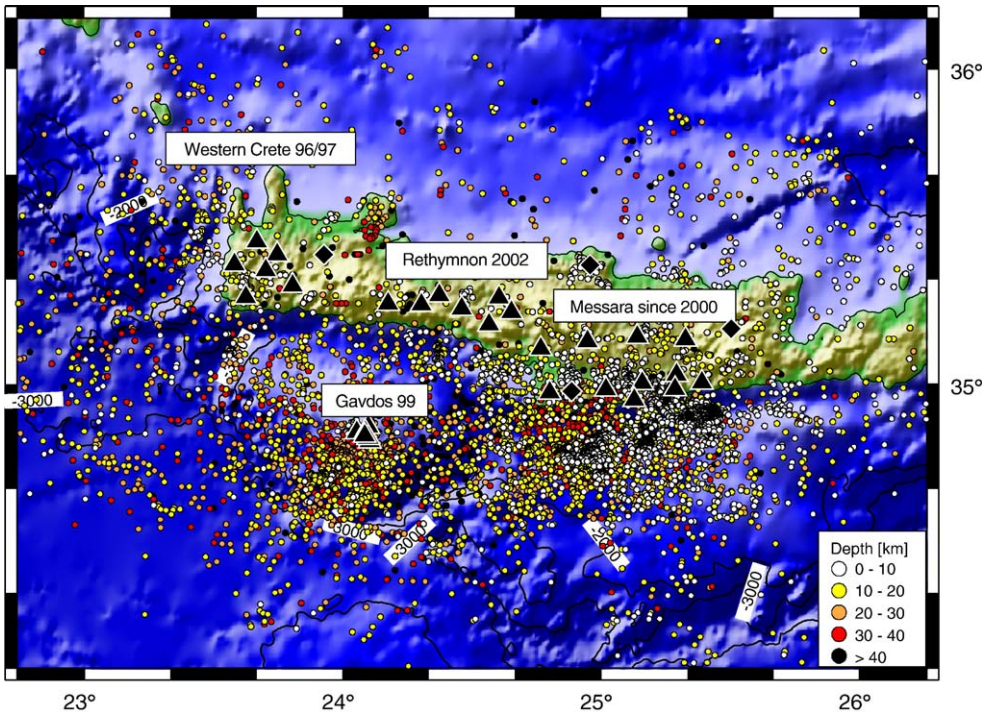

Fig. 2. Seismic activity located with the short period networks on Crete and Gavdos between 1996 and 2003 constituting database A. Also indicated are the station locations (black triangles) of the various networks and the GEOFON broadband stations (Hanka and Kind, 1994) which were incorporated in the data analysis (black diamonds).

In the current study we examine the characteristics of clusters found in the central Hellenic Subduction Zone. Clusters are investigated with respect to migration of their hypocenters and the possible influence of fluids on their generation. Their spatio-temporal pattern is discussed.

2. Data

The data were collected during the operation of temporary short period networks by the Ruhr University Bochum on the islands of Crete and Gavdos. Details about the networks installed between 1996 and 2001 as well as an evaluation of the microseismic activity observed are described by Meier et al. (2004). In this study we also include data gathered during a campaign in 2002 in the Rethymnon area. This network was intended to fill the gap in the observations between the networks on western Crete (1996) and in the Messara region (2000/1). From May 2003 until November 2004 the two south-eastern stations of the Messara network were reoccupied and three additional stations were installed at the southern shore of central Crete. The network's small aperture and its proximity to the Ptolemy structure were designed so that the previously detected cluster activity in this region could be mapped with higher resolution and with a lower detection threshold. The configurations of the various networks are shown in Fig. 2. The campaigns described by Meier et al. (2004) as well as the Rethymnon data were evaluated using a routine data processing scheme. All events detected were processed manually by picking P- and S-phases whenever possible and were then located using the hypo71 location software (Lee and Lahr, 1972). Hypocenter locations and P- and S-arrival times for these events were thus readily available.

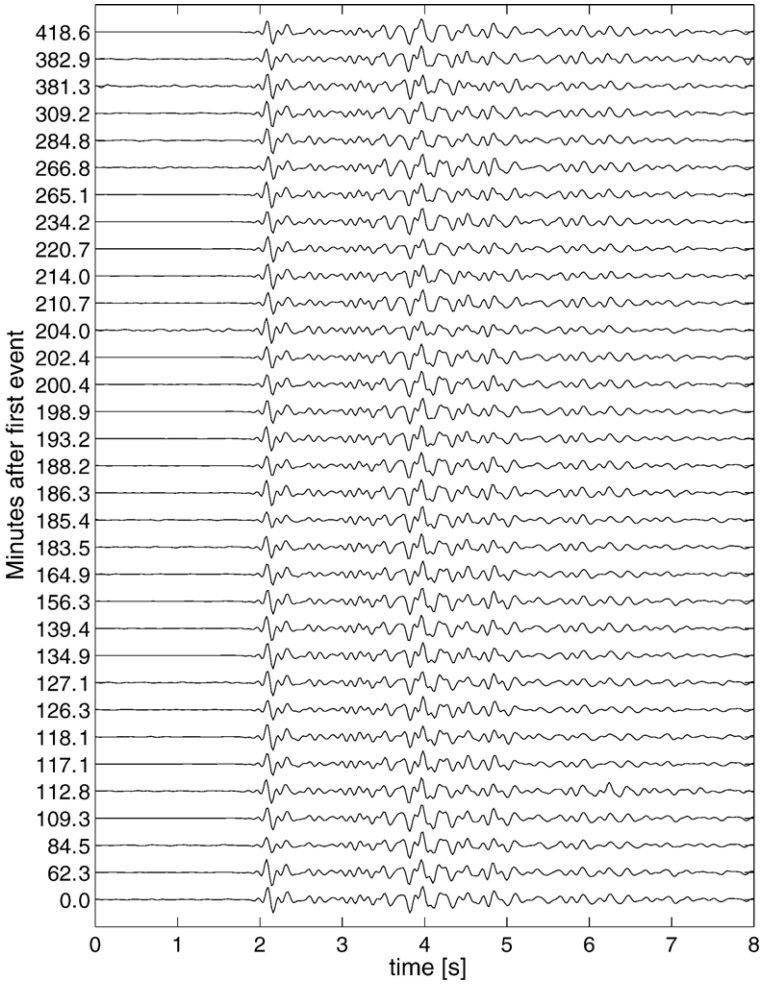

Fig. 3. Waveform example of a cluster recorded in 2000 at station M005 of the Messara network (Fig. 5b). Events belong to the cluster on Julian day 250 in 2000 (Figs. 4 and 5). The epicentral distance to the cluster which is located in the region of the southern shore line is approximately 12 km and the activity displayed here lasted for only 7 h.

For the 2003/4 network the processing scheme was automatized. Events were detected by applying a STA/LTA trigger and subsequently requiring at least three simultaneously triggered stations. The results were then reviewed to exclude remote events and the catalog was confined to events having S–P times of less than 8 s at at least one station. For the two main clusters in May and June 2003, however, all identifiable events were conventionally processed using hypo71. They were merged with the results from the routine processing for the years 1996–2002, resulting in a database containing 7299 hypocenters (see Fig. 2 for epicenter locations) and their corresponding P- and S-arrival times. This data set will be referred to as database A in the following. Furthermore, time series data from 4279 automatically processed events from the period May 2003–June 2004 with an S–P travel time of less than 8 s but without phase and hypocenter information were available for cross correlation. This database will be referred to as database B in the following.

3. Cluster analysis

3.1. Detection

In order to identify clusters of similar events waveform cross correlation was performed for each station. This was done for all events for which picked P- and S-phases from the respective station were present in database A. Because only data with identified P- and S-phases were considered, a high signal to noise ratio and a good data quality are assured for this dataset. Fig. 3 shows waveforms for a cluster consisting of 33 events recorded at a station of the Messara 2000/1 network within an interval lasting 7 h. Data filtered between 2 and 10 Hz and containing both P- and S-onset were used for all events in this database. The time window for cross correlation started 1 s before the picked P-arrival and lasted until $Tp + 1.8 * (Ts - Tp)$ (where Tp is the time of the P-arrival and Ts is the time of the S-arrival) thus constituting an adjustable window containing both the P- and S-arrivals. Correlating waveforms which contain information about the S–P time as well as the P- and S-wave ratios ensures close spatial proximity and similarity of source mechanism resulting in high correlation coefficients. See Fig. 3 for an example of similar waveforms found in this study.

Fig. 4 shows an example of a similarity matrix for events in southern central Crete and the adjacent offshore region recorded in 2000 at station M005 of the Messara network (Fig. 5b). This symmetric matrix contains the correlation coefficients of all possible event combinations at a single station. The matrix shows correlation coefficients for the chronologically ordered events shown in Fig. 5b. Clusters of similar events are detected which belong to episodal swarm-like activity

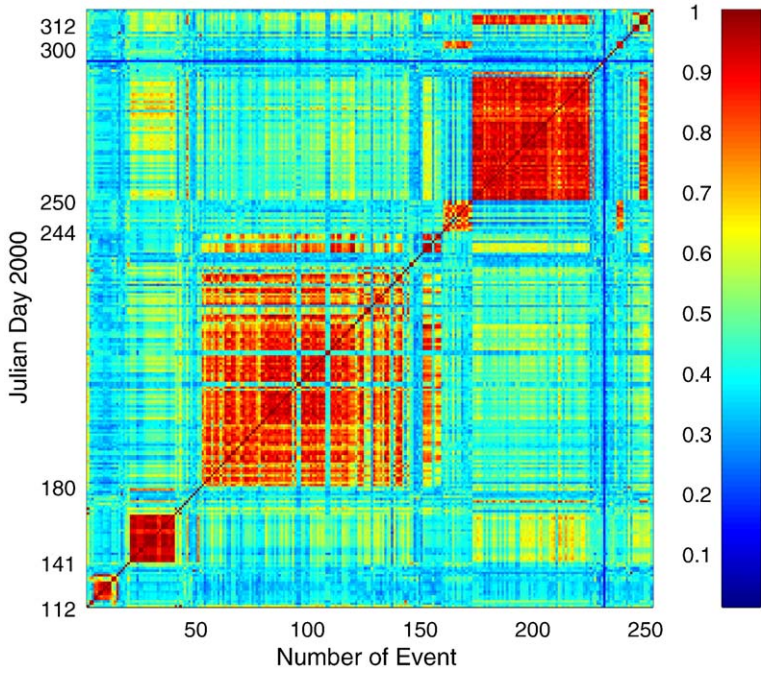

Fig. 4. Cross correlation matrix for the events shown in Fig. 5. Color scale indicates the correlation coefficient.

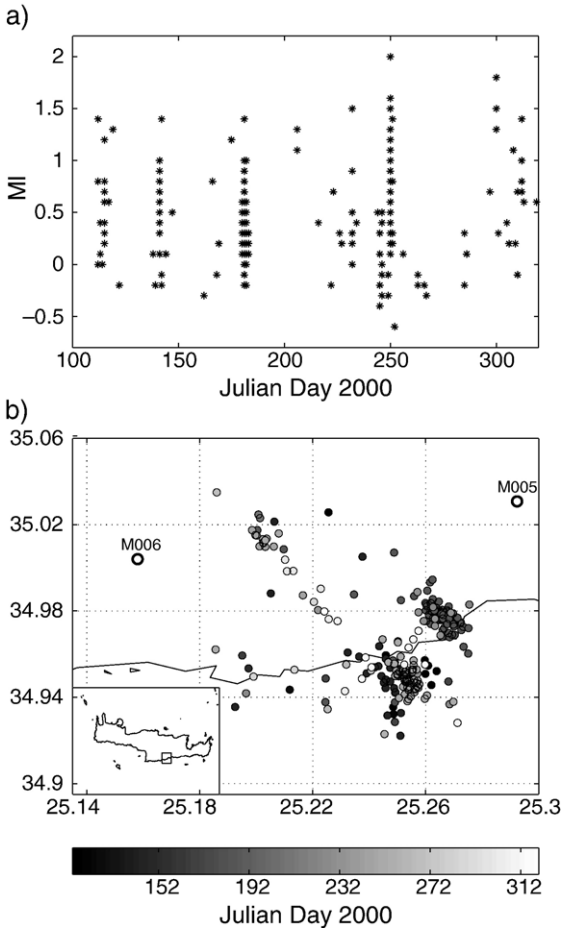

Fig. 5. Microseismic activity recorded with the Messara network in 2000 in the region of the southern Cretan shore. a) Magnitude–time plot of the events. b) Single event catalog locations of the microseismic activity. Gray shading with respect to time of occurrence.

(Fig. 5a) in distinct areas (Fig. 5b). These are typical of the cluster activity south of Crete. In a further processing step all available cross correlation coefficients for a specific event pair were stacked and for all pairs with at least 3 observations (i.e. at least three stations for which cross correlation coefficients were determined) average correlation coefficients were calculated. Only these events were considered in the further analysis of events present in database A.

The final association of an event to a specific cluster can be achieved either by a single, a complete or some intermediate linkage approach (Everitt, 1993; Aster and Scott, 1993). In these clustering schemes each event is initially regarded as a separate cluster. In the single linkage approach two clusters are always merged to form a new cluster when any two members of the different clusters exhibit a correlation coefficient larger than a threshold value. The complete linkage approach demands that this constraint is met by all possible event combinations. An intermediate approach may ask that a certain similarity threshold is met with respect to the mean correlation coefficient for all possible event pairs (Everitt, 1993). By definition a single linkage approach creates larger clusters than a complete linkage approach which on the other hand tends to create more but smaller clusters of highly similar events for the same threshold value. In this study a single linkage approach was used (Everitt, 1993; Aster and Scott, 1993) after initial trials with a complete linkage algorithm showed that many small, closely spaced clusters with highly similar waveforms active during the same time period were artificially separated by the clustering algorithm. The threshold of the cross correlation value was set to 0.9 after visual inspection of the cross correlation matrices and the waveforms belonging to the same cluster. By applying these processing steps to the data contained within database A we were able to identify a total of 315 multiplets with 1066 events. Most of the multiplets (210) consist of only 2 events (doublets) but 46 clusters have 5 or more members. The largest clusters consist of 33, 26 and 24 members, respectively.

The events in database B were analysed using a different approach due to the lack of P- and S-arrival times for them. Data for time windows of 50 s length were stored and in the first step the time lag for the highest cross correlation coefficient between two windows was determined. In a second step the time windows were shifted with respect to each other by this time lag and the maximum cross correlation coefficient of a time window lasting 10 s was calculated. As no adaptive windowing was used and no emphasis was put on data quality, correlation coefficients are generally lower than for data from database A. Nevertheless, this approach proved to be robust enough to identify clearly distinct clusters during the subsequent processing steps.

For the events in database B the station showing the best overall signal to noise ratio (SNR) was chosen as the reference station for which the cluster analysis was performed. For this station a cross correlation matrix was constructed containing all available events and the clustering algorithm was performed with a threshold value of 0.7. The cross correlation scheme was extended to this value lower than that used for events in database A, and the data processing automized as described in order to include events with lower SNR. In this way clusters consisting of weaker events could be detected by lowering the detection threshold. Although this increased the chance of misassociating individual events and thus merging actually distinct clusters, the procedure

proved to be robust. Visual inspection of all clusters with at least ten members showed that only one of them was created by incorrect linkage of actually distinct events. This cluster was subsequently broken into 2 smaller clusters and the misassociated events removed. This led to a total of 31 clusters each with at least 10 events for database B. For each cluster the event with the best SNR at the reference station was taken to be the master event. This event was located using waveforms from the stations of the Messara 2003/4 network.

3.2. Location

Locations of cluster centroids from database A are indicated in Fig. 6 by filled circles scaled to the number of members within each cluster. Obviously, the clusters are located throughout the study region with depths ranging from near the surface to more than 40 km. A major accumulation of clusters is evident off the southern shore of central Crete in the area of the Ptolemy trench. Of course this picture is enhanced by the fact that this region is part of the area with the longest observation period. The greatest cluster activity in this region is associated with a nearly vertically dipping structure in the region of the Ptolemy trench described by Meier et al. (2004). Most of the activity in this region is located at crustal depths pointing to processes within the continental Aeagean crust. In contrast, cluster activity below the island of Gavdos is deeper and considered to be part of the interplate seismicity between the subducting African lithosphere and the Aegean plate. Further activity is observed in the onshore region of central Crete as well as the south-western offshore region; for the latter the control on the hypocenter locations is lower due to the fact that these events are far outside the networks.

Results for database B are depicted in Fig. 6 by inverted triangles. The cluster activity is restricted to the region of the Ptolemy trench in the south, to a small area at the northern coast of Crete and to one spot in the Messara region where there are also clusters from database A. The distribution of clusters in the region of the Ptolemy trench supports the results from database A. This trench exhibits cluster activity along almost its entire length towards its north-eastern landward termination. While this activity is detected throughout the entire observation period at distinct locations, activity in the north is confined to a few days in 2003.

3.3. Characteristics

Clusters detected in this study generally exhibit swarm-like microseismic activity lasting for only a few hours or days (Fig. 5). The magnitude–time plot for events close to the southern shore in central Crete (Fig. 5a) shows that the seismic sequences are not dominated by a major event but in fact exhibit swarm-like behaviour which can be attributed to spatially distinct

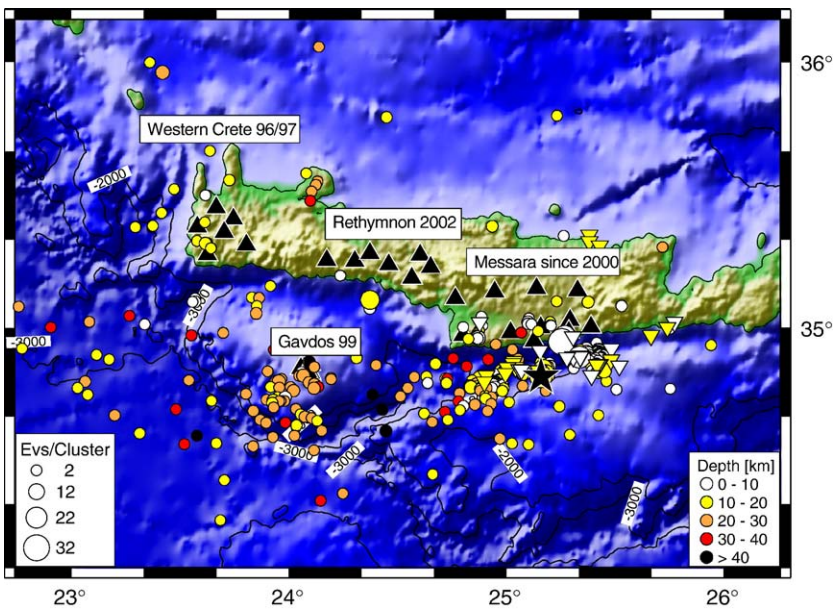

Fig. 6. Locations of all cluster centroids determined in this study. Circles denote centroids for clusters of database A while inverted triangles denote those of database B. Star marks the location of the relocated cluster in Fig. 8.

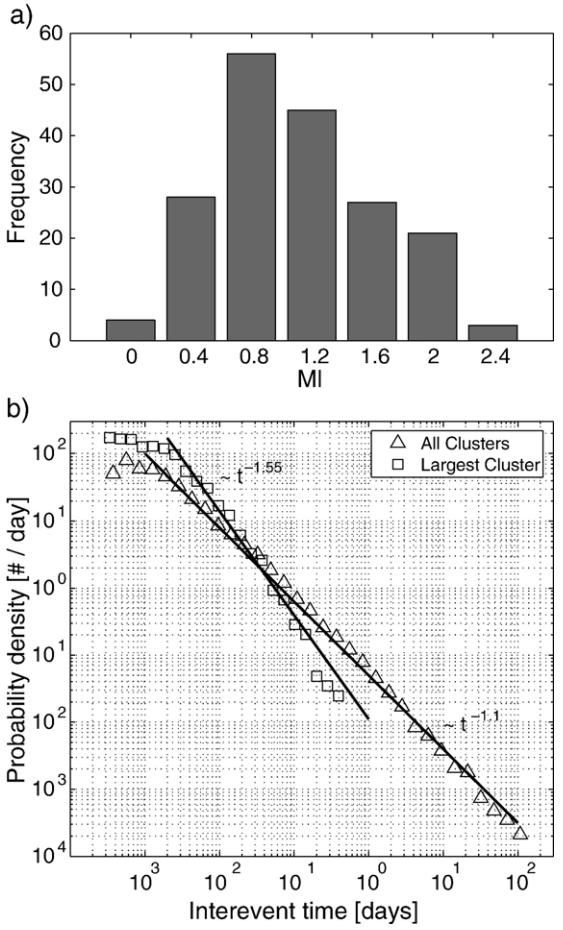

Fig. 7. a) Magnitude frequency distribution of the largest event within each cluster recorded during the 2000/1 Messara campaign. b) Interevent time probability distribution for all events belonging to the largest cluster (squares) and all cluster events in database A and B (triangles).

microseismic activity (Fig. 5b). The absence of larger events in clusters is also apparent in Fig. 7a. The histogram shows the magnitude frequency distribution for the largest event belonging to each cluster identified using data from the Messara 2000/1 campaign and thus constituting a data subset from database A. This observation also holds when considering all seismicity within a cluster region and not only the similar events of a single cluster.

Although occasionally a cluster may reactivate such behaviour is not characteristic for the clusters studied within the period of observation. Subtle differences in color for event pairs belonging to the same cluster in the similarity matrix of Fig. 4 hint at corresponding changes in their waveforms. These waveform differences may be attributed to a small change in hypocenter position or source characteristic and thus support the idea that we are not dealing with repeating events but an activity spanning a spatial extent of up to several hundreds of meters.

Fig. 7b shows the distribution of interevent times for events belonging to the same cluster. The double logarithmic plot is created by dividing the time axis into logarithmically scaled intervals, counting the number of interevent times between two successive events belonging to the same cluster within each interval and subsequently normalizing the number contained within each interval to one day. Squares in Fig. 7b are for successive interevent times of the largest cluster (Fig. 8) while triangles indicate the results for all clusters in database A and B. The distribution follows a power law with different slopes for events belonging to the largest cluster and all identified clusters combined. For events of the largest cluster a power law $\sim t^{-1.55}$ exists while the result for all cluster events combined suggests a power law $\sim t^{-1.1}$.

The well known Omori law (e.g. Utsu et al., 1995) which predicts an exponential decay in the number of aftershocks of major events with time shows a power law behaviour. Assuming that an aftershock sequence can be represented by a non-stationary Poisson process, Senshu (1959) showed that the interevent time distribution of the aftershock sequence also follows a

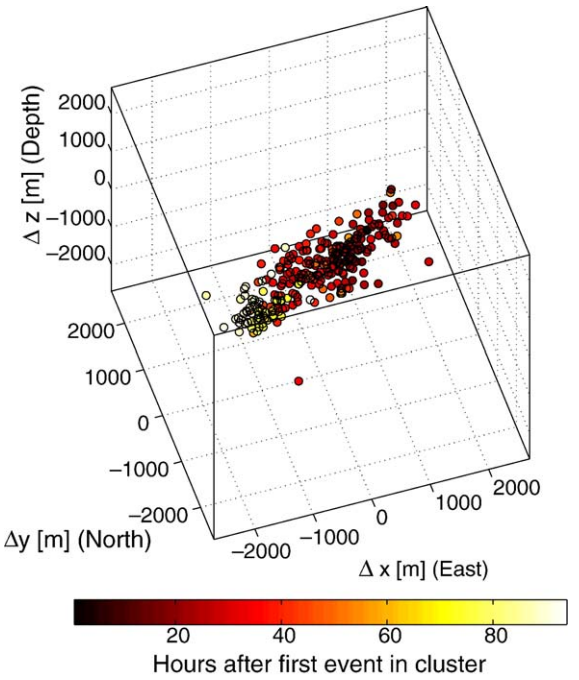

Fig. 8. Perspective view of relocated hypocenters belonging to the largest cluster depicted as star in Fig. 6 and showing hypocenter migration.

power law behaviour. Recently, Hainzl (2004) observed this power law behaviour of interevent times in seismic swarms in the Vogtland region (Hainzl, 2004). Seismic swarm activity in that region is generally linked to fluid intrusions (Spicak and Horalek, 2001; Hainzl, 2004). He was able to model the observed power law $\sim t^{-1.5}$ in a numerical simulation incorporating fluid diffusion and postseismic creep (Hainzl, 2004). Our findings for the Hellenic Subduction Zone support the idea of a power law behaviour of interevent times in seismic swarms.

4. Relative cluster relocation

The cluster analysis has revealed that adjacent clusters often exhibited seismic activity within the same time period. One possible explanation for this is a migration of the seismic activity between them. This can be tested by precise relative relocation of the hypocenters of the cluster events. To jointly investigate the behaviour of such closely spaced clusters, we decreased the correlation threshold to 0.7 while maintaining the requirement that the events be recorded by a minimum of three stations. Applying this approach to the data in database A merged previously distinct clusters to considerably larger entities and also created clusters which did not exist previously. The most prominent feature is a cluster containing more than 250 members in the Ptolemy region (star in Fig. 6). Further clusters with 30 to 160 members were also created by this approach and predominantly located in the same area.

For the relative relocation the program hypoDD (Waldhauser and Ellsworth, 2000) was used. While catalog times were taken directly from the routine processing, cross correlation times were calculated for the 30 nearest neighbours of each event. This was done in the time domain by resampling 50 Hz data to 1000 Hz and then finding the time lag for the highest cross correlation coefficient. This approach was performed for P- and S-arrivals separately with time windows of 1 s cut out from data bandpass filtered between 2 and 10 Hz. Only times with cross correlation coefficients larger than 0.65 were retained and the times were weighted according to their cross correlation coefficient.

Fig. 8 shows the result for the largest cluster. The activity began to the east of the cluster centroid and initially migrated toward the east and then toward the west. Later activity however was only recorded at the western end of the cluster. The cluster extends approximately 3 km in EW direction. The distance of 2 km from its point of initiation to its western

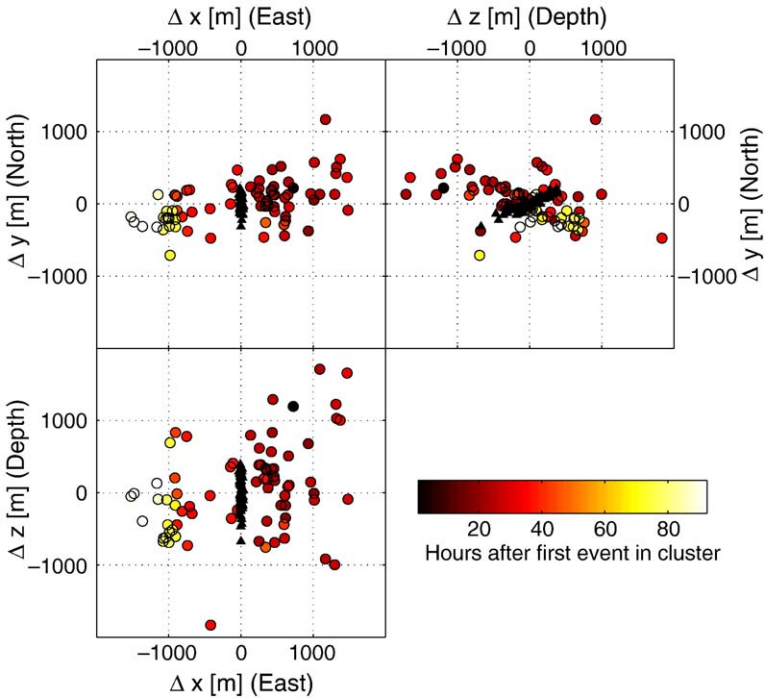

Fig. 9. Comparison of the best constrained hypocenters of the cluster in Fig. 8 (color coded circles) with the locations of synthetic hypocenters determined from exact travel times perturbed with realistic random errors (small black triangles).

termination was covered in a little less than 4 days suggesting a migration velocity of about 0.5 km per day.

In order to address the uncertainties in the locations of the relocated events, synthetic tests were performed. Exact travel times from the cluster centroid to the recording stations were perturbed with a realistic, normally distributed random error. Fig. 9 compares the results for 64 synthetic events initially located at the centroid of the largest cluster (black triangles) to locations of the 75 best constrained events (at least 10 cross correlation and catalog times per event pair) of this cluster (filled circles). The ENE-WSW elongation of the cluster which follows the trend of the Ptolemy trench in this region is in sharp contrast to the structure dipping from south to north obtained from the synthetic tests. This apparent structure clearly reflects the influence of the network configuration on the hypocenter distribution. The north–south vertical section in Fig. 9 hints at a fault-plane dipping steeply to the south which contrasts with the northward dipping structure created by the incorporation of random errors. Error estimates for the catalog locations in database A can be found in Meier et al. (2004) and are of the order of 5–10 km. However the maximum relative error for the relocated hypocenters inferred from the synthetic tests is in the range of 500 m for the least constrained axis of the error ellipsoid (Fig. 9).

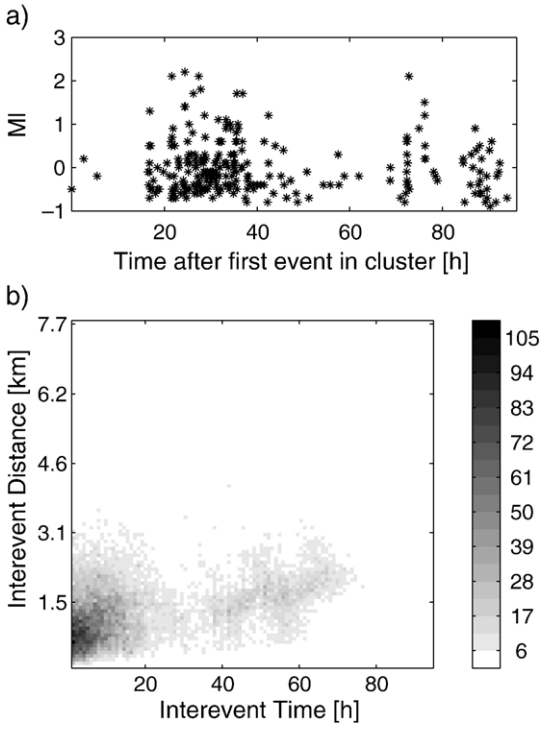

Fig. 10. a) Magnitude–time plot of the events forming the cluster in Fig. 8. b) Histogram of interevent distance versus interevent time for all possible event combinations of the cluster in Fig. 8. The shading indicates the number of event pairs that belong to the same bin.

Fig. 10a shows the magnitude–time plot for this cluster indicating embedded swarm activity consistent with the subclustering observed in the cluster analysis. It is also evident that the subclusters also behave like swarms without a dominant event. Fig. 10b displays a histogram of all possible event combinations for the cluster with the bins determined both by interevent distance and interevent time. The majority of event combinations plots just above the origin thus indicating events with a very short interevent time and a small offset in position. Repeating events would plot in the lowest row of Fig. 10b which represents an interevent distance of less than 100 m. This offset in the interevent distance increases with increasing interevent time. Furthermore, it is also possible to infer a feature with positive slope in this plot. It is especially pronounced in the interevent time range from 40 to 70 h representing the interval between the beginning of strong activity and the last two sub-swarms of Fig. 10a. The slope can be interpreted as the migration velocity of the hypocenters and is of the order of 500 m/day.

Migration of the microseismic activity over time was also observed to a lesser degree for two other clusters with much smaller spatial extents.

5. Discussion and conclusions

This study was aimed at finding clusters of events displaying a high degree of waveform similarity and obtaining quantitative measures for the event sequences forming these clusters. Because the results of the cluster analysis depend on the choice of threshold value for the cross correlation coefficient and the minimum number of stations required to meet this threshold value, changing these values will also change the results. The different threshold values and required numbers of stations meeting this value for database A and B, however, produced very similar results with respect to the spatio-temporal behaviour of the identified clusters. Thus, a careful analysis of the similarity matrices to find the appropriate cross correlation threshold value seems to be a viable approach.

The event sequences making up these clusters belong to the swarm type because most of the activity for a given cluster is limited to a short time interval and has no major events (Fig. 5). Although a seismic reactivation was observed for several regions, the events did not meet the necessary cluster criteria. The spatial and temporal extent of the different clusters varies. While

most clusters show microseismic activity confined to only a few hours and a spatial extent confined to hundreds of meters, occasionally a cluster occurs in which activity lasts for several days and the hypocenters tend to migrate from one center of activity to another (Fig. 8) covering distances of several kilometers. This behaviour is also observed in other regions with swarm-like activity and is related to the triggering effect of fluids (Parotidis et al., 2003).

The absence of repeating earthquake sequences in our analysis does not exclude the possibility of their occurrence in the study area. It merely shows the limitation of the data used in our analysis with its short recording periods of generally only a few months. This recording period may be too short to include the repeated occurrence of events forming a series of repeating events which generally show recurrence intervals of several months or years (Nadeau and McEvilly, 1997).

The presence of spatially and temporally distinct subclusters with higher correlation coefficients within larger clusters suggests the activation of different fault patches caused by a driving force which migrates. This pattern hints at a highly heterogeneous rupture surface. The possibility that distinct focal mechanisms due to the activation of differently oriented fault-planes create the subclustering is not supported by the distribution of the hypocenters for the largest cluster (Fig. 8) which seem to belong to the same fault-plane.

The decay in activity within a single cluster or subcluster follows an Omori law (Fig. 7)(Utsu et al., 1995) and may thus be linked to a stress triggering mechanism within the single cluster as it is evident for aftershock sequences (Stein, 1999). Such behaviour has also been observed and modelled for other regions with swarm activity triggered by fluids (Hainzl, 2004). The slight offset in interevent distances observable in Fig. 10b as well as subtle differences in the waveforms of events belonging to the same cluster suggest the activation of adjacent patches of the rupture surface. This contrasts with the idea of repeating events and can be explained with a decrease in shear stress at the ruptured fault patch making this now relaxed portion of the rupture surface less likely to break again. Such behaviour is reported in other studies (e.g. Rubin et al., 1999) as well, although cases of repeating events within aftershock sequences (Schaff and Beroza, 2004) have been observed as well.

The spatial distribution of clusters is not random but generally follows the observed distribution of microseismicity in the study area (Meier et al., 2004). The accretionary prism of the Hellenic Subduction Zone to the south exhibits aseismic deformation and compaction of the sediments with related mud volcanoes (Cifci et al., 1997; Kopf, 2002). The plate contact south of Crete shows strong microseismic activity between about 20 and 40 km depth (Meier et al., 2004) as well as intermediate magnitude activity (Engdahl et al., 1998) and may also have the potential to create major events (Papazachos et al., 2000). Cluster activity at depths compatible with the plate interface was located in the central forearc region of the Hellenic Subduction Zone, especially in the region of the island of Gavdos and the western part of the Ptolemy trench. Here depths up to more than 40 km indicate low seismic coupling in this depth range.

The eastern part of the Hellenic forearc consists of forearc slivers separated by the Ptolemy, Pliny and Strabo ‘trenches’ which were identified as deep-sea depressions with wedge-shaped sedimentary basins of up to 4 km thickness (Bohnhoff et al., 2001) that developed in a regime of sinistral transtension active in the region for the last approximately 3 Ma (ten Veen and Kleinspehn, 2003). Microseismic studies (Meier et al., 2004) identified a nearly vertical, seismically active structure reaching from the plate interface to near surface depths within the Ptolemy trench that may represent the contact between the forearc sliver and the Aegean lithosphere beneath Crete. This observation correlates with seismic studies which identified fault zones down to the mid-crustal reflector in that region (Bohnhoff et al., 2001). The cluster analysis identifies the Ptolemy trench as being very active, with nearly continuous cluster activity spanning its entire length and presumably also its entire depth from the lower continental crust to the surface (Fig. 6). Relocation of the largest cluster revealed a hypocenter migration following the strike of the Ptolemy trench. As the campaigns were limited to land-based stations, the question whether the Pliny and Strabo trenches show a similar behaviour cannot be addressed. The detection threshold is too high to quantify possible cluster activity at those distances. Following the subduction to greater depths in the north, microseismic and cluster activity ceases and we enter a domain of aseismic deformation. This might be explained by the serpentinization of the Aegean mantle due to the dehydration of the subducting African crust as suggested by receiver function studies in the region (Li et al., 2003).

The distribution of observed clusters might be linked to fluid circulation in the forearc of the Hellenic Subduction Zone. A model for such a circulation system

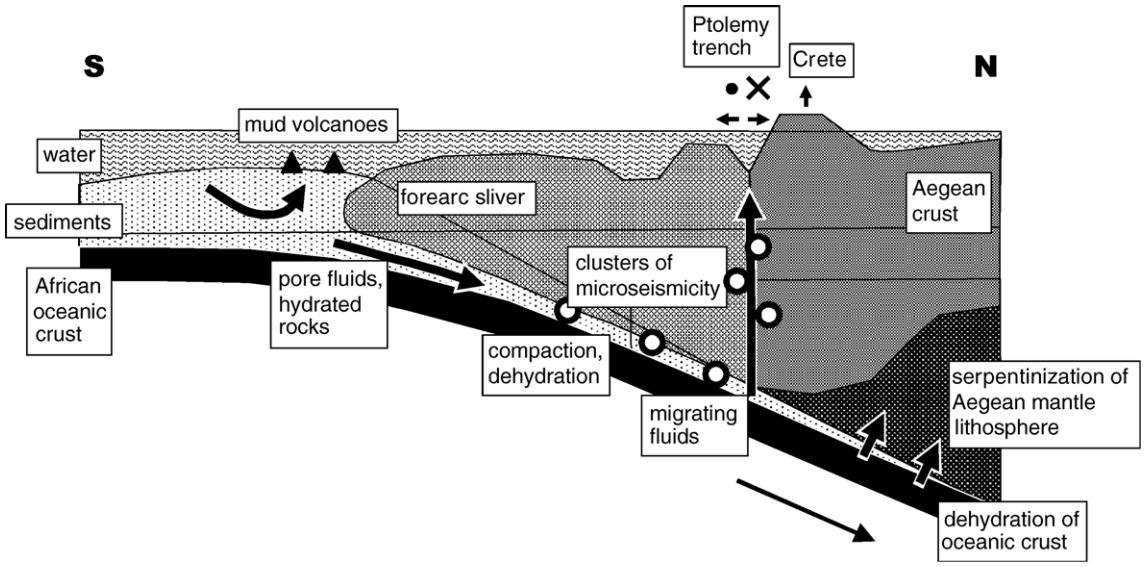

Fig. 11. Sketch of a model for fluid circulation in the Hellenic forearc region and associated cluster activity. Fluids contained within the sediments of the Libyan Sea are either expelled at mud volcanoes in the Mediterranean Ridge or subducted. The subsequent compaction of sediments or dehydration of the oceanic crust may trigger microseismic cluster activity at the plate interface while strong cluster activity points to ascending fluids in the Ptolemy structure.

is schematically sketched in Fig. 11. Some of the water contained within the thick sediment cover of the Libyan Sea is expelled in mud volcanoes of the accretionary prism (Cifci et al., 1997; Kopf, 2002) without detectable microseismic activity. Another portion of the water contained as pore fluids within the sediments or in the form of hydrated rock within the upper part of the oceanic crust is subducted. Increased pore pressure may cause the observed microseismic activity. Finally the transtensional Ptolemy structure may form a region of crustal weakness where the fluid ascends towards the surface triggering clusters of seismic events along its way. Detailed studies of the seafloor in the region of the Ptolemy trench could reveal the surfacial expressions of such fluid circulation. Below 40 km cluster activity and microseismicity cease, pointing to a change in the properties of the plate contact and a seismic decoupling of the plates at greater depth.

Acknowledgements

We greatfully acknowledge the cooperation with the university of Chania, especially N. Economou and A. Vafidis, during several field campaigns in the study area. The authors thank B. Klotz and L. Kühne for their help in the installation and maintenance of the networks and the GeoForschungZentrum Potsdam for the availability of waveform data through their GEOFON project. The cluster analysis was greatly aided by programs written by S. Baisch and the hypoDD relocation code was provided by F. Waldhauser. We thank S. Hainzl for useful discussion and comments. We wish to thank Peggy Hellweg and an anonymous reviewer for valuable comments and constructive criticism which helped to improve the manuscript. (Figs. 1, 2 and 6) were prepared using GMT software. The work was supported by the German Research Foundation (DFG) within the collobarative research center 526 “Rheology of the Earth: From the Upper Crust to the Subduction Zone”.

References

Aster, R.C., Scott, J., 1993. Comprehensive characterization of waveform similarity in microearthquake data sets. Bull. Seismol. Soc. Am. 83, 1307–1314.

Becker, D., 2000. Mikroseismizität und Deformation der Kruste Ostkretas, Master thesis, Faculty of Geophysics, Hamburg University (in German).

Becker, D., Meier, T., Bohnhoff, M., Harjes, H.-P., 2004. Seismic coupling between the Aegean and African lithosphere in the Hellenic Subduction Zone. Symposium Tectonics on Human Time Scale. Bochumer Geowissenschaftliche Arbeiten, vol. 3.

Bohnhoff, M., Makris, J., Stavrakakis, G., Papanikolaou, D., 2001. Crustal investigation of the Hellenic subduction zone using wide aperture seismic data. Tectonophysics 343, 239–262.

Cifci, G., Limonov, A., Dimitrov, L., Gaianov, V., 1997. Mud volcanoes and dome-like structures at the Eastern Mediterranean Ridge. Mar. Geophys. Res. 19, 421–438.

de Chabalier, J.B., Lyon-Caen, H., Zollo, A., Deschamps, A., Bernard, P., Hatzfeld, D., 1992. A detailed analysis of microearthquakes in

western Crete from digital three-component seismograms. Geophys. J. Int. 110, 347–360.
Delibasis, N., Ziazias, M., Voulgaris, N., Papapdopoulos, T., Stavrakakis, G., Papanasttassiou, D., Drakatos, 1999. Microseismic activity and seismotectonics of the Heraklion area (central Crete Island, Greece). Tectonophysics 308, 237–248.
Engdahl, E.R., van der Hilst, R., Buland, R., 1998. Global teleseismic earthquake relocation with improved travel times and procedures for depth determination. Bull. Seismol. Soc. Am. 88, 722–743.
Everitt, B.S., 1993. Cluster Analysis. Arnold, London.
Gillard, D., Rubin, A.M., Okubo, B., 1996. Highly concentrated seismicity caused by deformation of Kilauea's deep magma system. Nature 384, 343–346.
Got, J.-G., Frechet, J., Klein, F.W., 1994. Deep fault plane geometry inferred from multiplet relative relocation beneath the south flank of Kilauea. J. Geophys. Res. 99, 15375–15386.
Hainzl, S., 2004. Seismicity patterns of earthquake swarms due to fluid intrusion and stress triggering. Geophys. J. Int. 159, 1090–1096. doi:10.1111/j.1365-246X.2004.02463.x.
Hanka, W., Kind, R., 1994. The GEOFON Program. Ann. Geofis. 33, 1060–1065.
Hatzfeld, D., Besnard, M., Makropoulos, K., Hatzidimitriou, P., 1993. Microearthquake seismicity and fault-plane solutions in the southern Aegean and its geodynamic implications. Geophys. J. Int. 115, 799–818.
Hayashi, Y., Morita, Y., 2003. An image of a magma intrusion process inferred from precise hypocentral migrations of the earthquake swarm east of the Izu Peninsula. Geophys. J. Int. 153, 159–174.
Igarashi, T., Matsuzawa, T., Hasegawa, A., 2003. Repeating earthquakes in interplate aseismic slip in the northeastern Japan subduction zone. J. Geophys. Res. 108. doi:10.1029/2002JB001920.
Jenny, S., Goes, S., Giardini, D., Kahle, H.-G., 2004. Earthquake recurrence parameters from seismic and geodetic strain rates in the eastern Mediterranean. Geophys. J. Int. 157, 1331–1347. doi:10.1111/j.1365-246X.2004.02261.x.
Kopf, A.J., 2002. Significance of mud volcanism. Rev. Geophys. 40. doi:10.1029/2000RG000093.
Kreemer, C., Chamot-Rooke, N., 2004. Contemporary kinematics of the southern Aegean and the Mediterranean Ridge. Geophys. J. Int. 157, 1377–1392. doi:10.1111/j.1365-246X.2004.02270.x.
Kurz, J.H., Jahr, T., Jentzsch, G., 2004. Earthquake swarm examples and a look at the generation mechanism of the Vogtland/Bohemia earthquake swarm. Phys. Earth Planet. Inter. 142, 75–88.
Lambeck, K., 1995. Late Pleistocene and Holocene sea-level change in Greece and south-western Turkey: a separation of eustatic, isostatic and tectonic contributions. Geophys. J. Int. 122, 1022–1044.
Lee, W., Lahr, J., 1972. HYPO71: a computer program for determining hypocenter, magnitude and first motion pattern of local earthquakes. U.S. Geol. Surv. Open-File Report, pp. 75–311.
LePichon, X., Chamot-Rooke, N., Lallemant, S., 1995. Geodetic determination of the kinematics of central Greece with respect to Europe: implications for eastern Mediterranean tectonics. J. Geophys. Res. 100, 12675–12690.
Li, X., Bock, G., Vafidis, A., Kind, R., Harjes, H.-P., Hanka, W., Wylegalla, K., van der Meijde, M., Yuan, X., 2003. Receiver function study of the Hellenic subduction zone; imaging crustal thickness variations and the oceanic Moho of the descending African lithosphere. Geophys. J. Int. 155, 733–748.
McClusky, S., Ballassanian, S., Barka, A., Demir, C., Ergintav, S., Georgiev, I., Gurkan, O., Hamburger, M., Hurst, K., Kahle, H.-G., Kastens, K., Kekelidze, G., King, R., Kotzev, V., Lenk, O., Mahmoud, S., Mishin, A., Nadariya, M., Ouzounis, A., Paradissis, D., Peter, Y., Prilepin, M., Reilinger, R., Sanli, I., Seeger, H., Tealeb, A., Toksöz, M.N., Veis, G., 2000. Global Positionng System constraints on plate kinematics and dynamics in the eastern Mediterranean and Caucasus. J. Geophys. Res. 105, 5695–5719.
McKenzie, D.P., 1970. Plate tectonics of the Mediterranean region. Nature 226, 239–242.
Meier, T., Rische, M., Endrun, B., Vafidis, A., Harjes, H.-P., 2004. Seismicity of the Hellenic subduction zone in the area of western and central Crete observed by temporary local seismic networks. Tectonophysics 383, 149–169.
Meulenkamp, J.E., van der Zwaan, G.J., van Wamel, W.A., 1994. On Late Miocene to recent vertical motions in the Cretan segment of the Hellenic arc. Tectonophysics 234, 53–72.
Nadeau, R.M., Johnson, J.R., 1998. Seismological studies at Parkfield: IV. Moment release rates and estimates of source parameters for small repeating earthquakes. Bull. Seismol. Soc. Am. 88, 790–814.
Nadeau, R.M., McEvilly, T.V., 1997. Seismological studies at Parkfield: V. Characteristic microearthquake sequences as fault-zone drilling targets. Bull. Seismol. Soc. Am. 87, 1463–1472.
Nadeau, R.M., Foxall, W., McEvilly, T.V., 1995. Clustering and periodic recurrence of microearthquakes on the San Andreas fault near Parkfield. Science 267, 503–507.
North, R.G., 1974. Seismic slip rates in the Mediterranean and Middle East. Nature 252, 560–563.
Papadopoulos, G.A., 1989. Seismic and volcanic activities and aseismic movements as plate motion components in the Aegean area. Tectonophysics 167, 31–39.
Papazachos, B.C., Comninakis, P.E., Karakaisis, B.G., Karakostas, B. G., Papaioannou, C.A., Papazachos, C.B., Scordilis, E.M., 2000. A Catalog of Earthquakes in Greece and Surrounding Area for the Period 550BC–1999. Geophysics Laboratory, University of Thessaloniki.
Parotidis, M., Rothert, E., Shapiro, S.A., 2003. Pore-pressure diffusion: a possible triggering mechanism for the earthquake swarms 2000 in Vogtland/NW-Bohemia, central Europe. Geophys. Res. Lett. 30. doi:10.1029/2003GL018110.
Rubin, A.M., Gillard, D., Got, J.-L., 1999. Streaks of microearthquakes along creeping faults. Nature 400, 635–641.
Schaff, D.P., Beroza, G.C., 2004. Coseismic and postseismic velocity changes measured by repeating events. J. Geophys. Res. 109. doi:10.1029/2004JB003011.
Senshu, T., 1959. On the time interval distribution of aftershocks. Zisin, Ser. 2 (12), 149–161 (in Japanese).
Shearer, P.M., 2002. Parallel fault strands at 9-km depth resolved on the Imperial Fault, Southern California. Geophys. Res. Lett. 29, 19–22.
Spicak, A., Horalek, J., 2001. Possible role of fluids in the process of earthquake swarm generation in the West Bohemia/Vogtland seismoactive region. Tectonophysics 366, 151–161.
Stein, R.S., 1999. The role of stress-transfer in earthquake occurrence. Nature 402, 605–609.
Stiros, S.C., 2001. The AD 365 Crete earthquake and possible seismic clustering during the fourth to sixth centuries AD in the Eastern Mediterranean: a review of historical and archaelogical data. J. Struct. Geol. 23, 545–562.
ten Veen, J.H., Kleinspehn, K.L., 2003. Incipient continental collision and plate-boundary curvature: Late Pliocene-Holocene transtensional Hellenic forearc, Crete, Greece. J. Geol. Soc. 160, 161–181.

Utsu, T., Ogata, Y., Matsu'ura, R.S., 1995. The centenary of the Omori formula for a decay law of aftershock activity. J. Phys. Earth 43, 1–33.

Waldhauser, F., Ellsworth, W.L., 2000. A double difference earthquake location algorithm: method and application to the Northern Hayward Fault. Bull. Seismol. Soc. Am. 90, 1353–1368.

Yamashita, T., 1999. Pore creation due to fault slip in a fluid-permeated fault zone and its effects on seismicity: generation mechanism of earthquake swarm. Pure Appl. Geophys. 155, 625–647.